NIH Public Access
Author Manuscript
*J Phys Chem Lett*. Author manuscript; available in PMC 2013 August 02.

Published in final edited form as:
*J Phys Chem Lett*. ; 3(15): 2030–2034. doi:10.1021/jz300742w.

# Dynamic Nuclear Polarization of Oxygen-17

**Vladimir K. Michaelis**[1], **Evgeny Markhasin**[1], **Eugenio Daviso**[1,2], **Judith Herzfeld**[2], and **Robert G. Griffin**[1]

[1]Francis Bitter Magnet Laboratory and Department of Chemistry, Massachusetts Institute of Technology, Cambridge, Massachusetts, USA, 02139

[2] Department of Chemistry, Brandeis University, Waltham, Massachusetts, USA, 02454

## Abstract

Oxygen-17 detected DNP NMR of a water/glycerol glass enabled an 80-fold enhancement of signal intensities at 82 K, using the biradical TOTAPOL. The >6,000-fold savings in acquisition time enables $^{17}$O-$^{1}$H distance measurements and heteronuclear correlation experiments. These experiments are the initial demonstration of the feasibility of DNP NMR on quadrupolar $^{17}$O.

### Keywords

DNP; water; NMR; cross-effect; HETCOR; CPMG; $^{17}$O

Recent years have seen an avalanche of new magic angle spinning (MAS) NMR methods developed to determine structures of macromolecular systems that are not amenable to study by either solution NMR or diffraction techniques, the two principle tools of structural chemistry. In particular, with MAS NMR there are now established methods to assign spectra and to perform distance and torsion angle measurements for the I=1/2 species $^{1}$H, $^{13}$C, $^{15}$N and $^{31}$P.[1,2] This in-turn has enabled studies of protein and nucleic structures and dynamics. Largely missing from the biomolecular NMR repertoire is oxygen, a key element of water and a variety of other chemically and biologically important functional groups. The difficulty is that the most abundant oxygen isotope, $^{16}$O, has no magnetic moment and the next most abundant, $^{17}$O, has a quadrupolar nucleus (I=5/2), with attendant spectral complications. On the other hand, $^{17}$O chemical shifts span ~1000 ppm with the potential for chemically significant spectral resolution. Two recent examples showed that the $^{17}$O shifts of carboxyl groups are dispersed over 60 ppm[3] and that the –C$^{17}$O$_2$ shift tensor elements are sensitive to H-bonding and span ~550-600 ppm[4].

Progress in $^{17}$O NMR has been stymied primarily by the low sensitivity resulting from the broad 2$^{nd}$ order powder patterns and low resolution of the spectra. This problem is further exacerbated by the low efficiency of the techniques used to observe $^{17}$O. In more detail, $^{17}$O MAS spectra display residual 2$^{nd}$ order broadening characteristic of a 4$^{th}$ rank tensor that is not averaged to zero by MAS [5,6]. To observe isotropic chemical shifts in the presence of and convolved with the 2$^{nd}$ order interaction requires either special instrumentation, as in case of

Correspondence to: Robert G. Griffin.

**Corresponding Author**rgg@mit.edu.

Author Contributions
The manuscript was written through contributions of all authors. / All authors have given approval to the final version of the manuscript.

**Supporting Information Available**. Materials and Methods, and Figure S1. This material is available free of charge via the internet http://pubs.acs.org.

NIH-PA Author Manuscript
NIH-PA Author Manuscript
NIH-PA Author Manuscript

NIH-PA Author Manuscript

NIH-PA Author Manuscript

NIH-PA Author Manuscript

double rotation (DOR) and dynamic-angle spinning (DAS)[7,8], or special spectroscopic techniques, as in case of multiple-quantum magic angle spinning (MQMAS)[9] and or satellite-transition magic angle spinning (STMAS)[10]. However, when the quadrupole coupling is large (> 5 MHz) the excitation efficiency of these approaches drops dramatically; in the case of MQMAS spectra, to about ~5% [11,12]. Thus, although there are a number of exciting MQMAS studies of $^{17}O$ labeled biological samples, the experimental results are clearly limited by signal-to-noise[3,13-20]. In order to enable $^{17}O$ NMR as an important spectroscopic technique, a dramatic increase in sensitivity is required.

Recently, high frequency dynamic nuclear polarization (DNP) has provided immense gains in NMR sensitivity via microwave-induced transfer of polarization from paramagnetic centers to nuclei [21]. In general, $^{1}H$'s are polarized directly and then cross-polarization is used to transfer the enhanced polarization to other nuclei (e.g., $^{13}C$, $^{15}N$, etc.), all at cryogenic temperatures (~85 K).[22-28] This approach has been successfully applied to membrane proteins[29-31] , peptides[32,33], amyloid fibrils[34] as well as surfaces[35,36]. Most of these studies focus on I=1/2 nuclei (e.g., $^{13}C$, $^{31}P$, $^{29}Si$, etc.) and a few on the I=1 and 5/2 quadrupolar species [35-37]. The magnetization transfer yields enhancements $\varepsilon$ = 30-250, and the low temperature yields another gain of ~3.5 in Boltzmann polarization relative to ambient temperature. In combination, $\varepsilon^{\dagger}$~105-875, which could dramatically improve the prospects of performing $^{17}O$ experiments in biological systems.

Here we demonstrate the feasibility of this approach in the simple case of $H_2{}^{17}O$. We observe for the first time an enhancement of $\varepsilon$~80 or $\varepsilon^{\dagger}$~280 for $^{17}O$ using high field DNP NMR and the polarizing agent TOTAPOL in a glassy glycerol/$D_2O$/$H_2O$ matrix. In particular we are able to polarize $^{17}O$ for both echo and Carr-Purcell-Meiboom-Gill (CPMG) [38] experiments and to use spin-echo double resonance (SEDOR) [39,40] experiments to measure $^{1}H$-$^{17}O$ distances. The dramatic savings in acquisition time demonstrates a potentially important approach to $^{17}O$ spectroscopy that can be extended to studies of $H_2{}^{17}O$ in other chemical systems and of $^{17}O$ in other functional groups.

Figure 1 shows a series of central transition (1/2 → -1/2) 1D spectra demonstrating DNP enhancements of $^{17}O$. Spectra acquired with a cross polarization (CP) echo experiment with and without microwave irradiation are shown in Figure 1b and 1e, respectively. The wave on-signal was acquired with ~20 minutes of signal averaging and the wave off-signal was acquired over a period of 14 hours with acquisition parameters identical to those for the on-signal. Comparison of the two yields $\varepsilon$~80.

The shape of the static powder pattern shown in Figure 1b is characteristic of a second-order quadrupolar coupling pattern [41-43]. Chemical shielding anisotropy can also influence the lineshape, although, for water at 5 T, this effect is negligible compared to that of the quadrupolar interaction. The quadrupolar coupling constant, $C_Q$ = 6.8 ± 0.2 MHz, the asymmetry parameter, • = 0.95 ± 0.05 and the isotropic chemical shift, $\delta_{iso}$ = 0 ± 50 ppm were determined by simulating the non-spinning powder pattern (Figure 1a). The sizeable quadrupolar coupling is reasonable for a frozen water environment. [44] The ~85 kHz breadth of the central transition limits the ability to use magic-angle spinning (MAS). In particular, the water/glycerol oxygen site at 5 T would require $\omega_r/2\pi$ > 30 kHz to isolate the central transition from a series of rotational sidebands. Current spinning frequencies with 4 mm rotors at cryogenic temperatures are limited to ~7 kHz due to the density of the $N_2$ drive and bearing gases being near the liquefaction point (T = 77 K). As DNP NMR instruments are developed for higher fields, lower spinning frequencies could suffice due to the inverse relationship between the breadth of the second-order quadrupolar interaction and $B_0$. For example, at 14 T, $\omega_r/2\pi$ = 10 kHz would be sufficient for $^{17}O$ MAS DNP experiments. Simulations illustrating this point are included in the Supporting Information.

NIH-PA Author Manuscript

NIH-PA Author Manuscript

NIH-PA Author Manuscript

CPMG experiments can provide higher signal-to-noise ratios by splitting the broad quadrupolar powder pattern into a series of sharp spikes,[38,45-49] and Figure 1c shows that DNP-enhanced CPMG can further accelerate the acquisition of $^{17}O$ spectra. A standard echo provided sufficient signal-to-noise with enrichment on the order of 10% or more; however CPMG proves to be useful for natural abundance (0.038%) $H_2O/D_2O$/glycerol glasses (Figure S1). This may enable future studies using low-levels of enrichment. DNP and CPMG might usefully be coupled to other sequences for quadrupolar nuclei and species that show large chemical shielding anisotropies if $T_2$'s are sufficiently long. Care must be taken when multiple sites are present, as different $T_2$'s could complicate spectral interpretation. Radical concentration can also compromise the CPMG method by paramagnetic relaxation. In Figure 1c, a train of 128 echoes, provided a signal beyond 11 ms. This indicates that, in this system, 20 mM of the biradical TOTAPOL[50,51] (or 40 mM electrons) had little effect on the spectrum (i.e., the breadth of the central transition is dominated by the quadrupolar line-shape). The build-up time constant ($\tau_B$) for the water/glycerol glass was experimentally determined to be 4.1 s.

The low sensitivity of $^{17}O$ NMR often requires weeks of acquisition time, rendering multidimensional structural experiments impractical. In consequence, most distances measured between $^{17}O$ and either $^{1}H$ or $^{13}C$ by NMR are indirect, applying a dephasing pulse on $^{17}O$ and observing $^{1}H$ or $^{13}C$. [47,48,52,53] In Figure 2 we show the results of a SEDOR experiment used to measure the average $^{1}H$-$^{17}O$ distance in the glycerol/water glass. A 1D stepped-SEDOR experiment was used to acquire a $^{17}O$[54] ($1-S/S_o$) curve characteristic of the dipolar coupling (Figure 2a).

The SEDOR curve was simulated using SIMPSON [52] and SPINEVOLUTION [55] software and is compared in Figure 2a with the experimental curve determined from the peak areas. Various spin models included a single oxygen site with 2-5 $^{1}H$'s between 0.8 and 1.2 Å and <HOH angles between $100^0$ to $110^0$ (values were chosen based on upper and lower limits of the experimental data). These inputs were adjusted until a reasonable model of the glass was obtained. A three-spin model (one - O and two – H's) indicated an average H---O bond distance of 1.1 ± 0.1 Å, a value that agrees well with X-ray and neutron diffraction data from various crystalline ice structures where H--O distances are found between 0.86 and 1.15 Å. [56-58]

A second Fourier transformation of the evolution dimension of the same SEDOR experiment yields a 2D dipole-quadrupolar correlation spectrum (Figure 2b) similar to those reported previously [59,60]. This spectrum is sensitive to the relative orientation of the dipole and quadrupolar tensors, and this information, in principle, can be extracted by fitting the experimental data. [59]

We found it to be difficult to achieve acceptable agreement between the experimental and simulated spectra. This difficulty can be attributed to the following two reasons. First, the samples used for all experiments were in the glassy state. Therefore, there must be a certain degree of structural disorder present (e.g., distance, angle and possibly coordination). Second, mobile protons were significantly diluted with deuterons, which come from deuterated glycerol and $D_2O$ used for sample preparation. Therefore, the observed 1D and 2D experiments have contributions from $^{17}O$ sites with varying number of neighboring protons. In the 2D SEDOR, the $^{17}O$-$^{1}H$ heteronuclear dipolar coupling can be estimated from the dipolar dimension[61]. The observed splitting of 16.3 ± 0.3 kHz, corresponds to a one bond distance of ~1 Å.

DNP NMR enables SEDOR experiments to measure single $^{17}O$ bond lengths within hours. This could be extended to $^{17}O$-$^{13}C$ or $^{17}O$-$^{15}N$ bond distances with appropriate hardware

NIH-PA Author Manuscript

NIH-PA Author Manuscript

NIH-PA Author Manuscript

and to other sequences, such as rotational echo double resonance (REDOR) and transferred echo double resonance (TEDOR), with higher field DNP. Experimental times for the identical experiments without DNP are projected to require >1.4 years.

Multidimensional experiments also enable the extraction of structural information by correlating resonance(s) from one NMR nucleus to another, through either the dipolar or J-coupling interactions. Figure 3 shows a $^{17}O$-$^{1}H$ heteronuclear correlation spectrum (HETCOR) for a water/glycerol glass. A projection along the $^{17}O$ dimension yields the quadrupolar pattern similar to Figure 1b. The indirect dimension ($^{1}H$) exhibits a broad resonance dominated by $^{1}H$-$^{1}H$ homonuclear dipolar coupling. $^{1}H$ chemical shielding and heteronuclear dipolar coupling are also present, although they contribute minimally to the observed lineshape.

For quadrupolar NMR, a 16-phase cycle is often used during acquisition of one- and two-dimensional data often leading to improved quadrupolar lineshapes. With the sensitivity boost from DNP and CPMG, a HETCORCPMG spectrum of the water/glycerol glass was also acquired using a 8 scan, 8-phase cycle acquisition scheme (not shown). The reduced phase cycle (versus 16) provided similar results, with only minor variations within the discontinuities. With the use of hard pulses, increased field ($B_o$) strength and studying systems with lineshapes below 80 kHz, this could provide an alternative for multidimensional experiments. Further reducing acquisition time for broad resonances and low sensitivity.

In summary, DNP in the simple case of $H_2{}^{17}O$ provided an enhancement of 80. Water is of great importance in both biological and chemical processes, but is challenging to study using conventional $^{17}O$ solid state NMR. The ability to polarize protons by microwave irradiation followed by cross-polarization to oxygen has enabled a suite of multi-dimensional NMR experiments of this low-gamma, quadrupolar nucleus within hours. $^{17}O$-detected multidimensional spectra were acquired between three and 10 hours using DNP NMR. By enhancing the signal-to-noise ratio, DNP provides an ~6,000-fold gain in time at cryogenic temperatures, and, in the absence of relaxation, a >18,000-fold gain in time compared to room temperature (298 K). These gains should be transferable to other difficult quadrupolar nuclei, providing a savings in acquisition time. The significant gain in sensitivity and reduction of experimental time from months to hours is extremely beneficial and provides new possibilities for further exploration of heteronuclear correlations and distances in multidimensional experiments. Extensions to MAS experiments for site assignments are currently in progress [62].

## Supplementary Material

Refer to Web version on PubMed Central for supplementary material.

## Acknowledgments

Research reported in this publication was supported by the National Institute of Biomedical Imaging and Bioengineering of the National Institute of Health under award numbers EB-001960, EB-002804, EB-001035, and EB-002026. VKM is grateful to the Natural Sciences and Engineering Research Council of Canada for a Postdoctoral Fellowship. We thank our colleagues Dr. G. Debelouchina, Dr. B. Corzilius, Dr. A. Smith, T.C. Ong and J. Bryant for their assistance and stimulating conversations during the course of this research.

Funding Sources

NIH EB-001960, EB-001035, EB-002804 and EB-002026

NIH-PA Author Manuscript

NIH-PA Author Manuscript

NIH-PA Author Manuscript

## REFERENCES


1. Rienstra CM, Hohwy M, Hong M, Griffin RG. 2D and 3D N-15-C-13-C-13 NMR Chemical Shift Correlation Spectroscopy of Solids: Assignment of MAS Spectra of Peptides. Journal of the American Chemical Society. 2000; 122:10979–10990.
2. Reif B, Jaroniec CP, Rienstra CM, Hohwy M, Griffin RG. H-1-H-1 MAS Correlation Spectroscopy and Distance Measurements in a Deuterated Peptide. J. Magn. Reson. 2001; 151:320–327. [PubMed: 11531354]
3. Wong A, Howes A, Yates J, Watts A, Anupold T, Past J, Samoson A, Dupree R, Smith M. Ultra-High Resolution (17)O Solid-State NMR Spectroscopy of Biomolecules: A Comprehensive Spectral Analysis of Monosodium L-Glutamate Center Monohydrate. Phys. Chem. Chem. Phys. 2011; 13:12213–12224. [PubMed: 21603686]
4. Waddell KW, Chekmenev EY, Wittebort RJ. Peptide 17O Chemical Shielding and Electric Field Gradient Tensors. J. Phys. Chem. B. 2006; 110:22935–22941. [PubMed: 17092047]
5. Grandinetti PJ. High Resolution Solid-State NMR of Quadrupolar Nuclei. Experimental NMR Conference Daytona Beach. 2007:1–38.
6. Grandinetti PJ, Trease NM, Ash JT. Symmetry Pathways in Solid-State NMR. Prog. NMR Spect. 2011; 59:121–196.
7. Chemlka B, Mueller K, Pines A, Stebbins J, Wu Y, Zwanziger J. O-17 NMR in Solids by Dynamic Angle Spinning and Double Rotation. Nature. 1989; 339:42–43.
8. Baltisberger JH, Gann SL, Grandinetti PJ, Pines A. Cross-Polarization Dynamic-Angle Spinning Nuclear Magnetic Resonance of Quadrupolar Nuclei. Mol. Phys. 1994; 81:1109–1124.
9. Frydman L, Harwood JS. Isotropic Spectra of Half-Integer Quadrupolar Spins from Bidimensional Magic-Angle Spinning NMR. J Am Chem Soc. 1995; 117:5367–5368.
10. Gan Z. Isotropic NMR Spectra of Half-Integer Quadrupolar Nuclei Using Satellite Transitions and Magic-Angle Spinning. J. Am Chem. Soc. 2000; 122:3242–3243.
11. Wu G, Rovnyak D, Griffin RG. Quantitative multiple-quantum magic-angle-spinning NMR spectroscopy of quadrupolar nuclei in solids. Journal of the American Chemical Society. 1996; 118:9326–9332.
12. Wu G, Rovnyak D, Huang PC, Griffin RG. High-Resolution Oxygen-17 NMR Spectroscopy of Solids by Multiple-Quantum Magic-Angle-Spinning. Chemical Physics Letters. 1997; 277:79–83.
13. Brinkmann A, Kentgens APM. Proton-Selective 17O-1H Distance Measurements in Fast Magic-Angle-Spinning Solid-State NMR Spectroscopy for the Determination of Hydrogen Bond Lengths. J.Am.Chem.Soc. 2006; 128:14758–14759. [PubMed: 17105257]
14. Gullion T, Yamauchi K, Okonogi M, Asakura T. 13C-17O REAPDOR NMR as a Tool for Determining Secondary Structure in Polyamides. Macromolecules. 2007; 40:1363–1365.
15. Hung I, Uldry A-C, Becker-Baldus J, Webber AL, Wong A, Smith ME, Joyce SA, Yates JR, Pickard CJ, Dupree R, Brown SP. Probing Heteronuclear 15N-17O and 13C-17O Connectivities and Proximities by Solid-State NMR Spectroscopy. Journal of the American Chemical Society. 2009; 131:1820–1834. [PubMed: 19138069]
16. Sefzik TH, Houseknecht JB, Clark TM, Prasad S, Lowary TL, Gan Z, Grandinetti PJ. Solid-State 17O NMR in Carbohydrates. Chem. Phys. Lett. 2007; 434:312–315.
17. Wong A, Beevers AJ, Kukol A, Dupree R, Smith ME. Solid-State 17O NMR Spectroscopy of a Phospholemman Transmembrane Domain Protein: Implications for the Limits of Detecting Dilute 17O Sites in Biomaterials. Solid State Nuclear Magnetic Resonance. 2008; 33:72–75. [PubMed: 18502619]
18. Wu G, Dong S, Ida R, Reen N. A Solid-State 17O Nuclear Magnetic Resonance Study of Nucleic Acid Bases. J.Am.Chem.Soc. 2002; 124:1768–1777. [PubMed: 11853455]
19. Yamauchi K, Okonogi M, Kurosu H, Tansho M, Shimizu T, Gullion T, Asakura T. High Field 17O Solid-State NMR Study of Alanine Tripeptides. J. Magn. Reson. 2008; 190:327–332. [PubMed: 18060815]
20. Zhu J, Ye E, Terskikh V, Wu G. Solid-State 17O NMR Spectroscopy of Large Protein-Ligand Complexes. Angewandte Chemie, International Edition. 2010; 49:8399–8402.

NIH-PA Author Manuscript

NIH-PA Author Manuscript

NIH-PA Author Manuscript


21. Carver TR, Slichter CP. Polarization of Nuclear Spins in Metals. Physical Review. 1953; 92:212–213.
22. Bajaj VS, Farrar CT, Hornstein MK, Mastovsky I, Vieregg J, Bryant J, Elena B, Kreischer KE, Temkin RJ, Griffin RG. Dynamic Nuclear Polarization at 9T Using a Novel 250 GHz Gyrotron Microwave Source. J. Mag. Res. 2003; 160:85–90.
23. Becerra LR, Gerfen GJ, Temkin RJ, Singel DJ, Griffen RG. Dynamic Nuclear Polarization with a Cyclotron Resonance Maser at 5 T. Phys. Rev. Lett. 1993; 71:3561–3564. [PubMed: 10055008]
24. Gerfen GJ, Becerra LR, Hall DA, Griffin RG, Temkin RJ, Singel DJ. High frequency (140 GHz) Dynamic Nuclear Polarization: Polarization Transfer to a Solute in Frozen Aqueous Solution. J. Chem. Phys. 1995; 102:9494–9497.
25. Hall DA, Maus DC, Gerfen GJ, Inati SJ, Becerra LR, Dahlquist FW, Griffin RG. Polarized-Enhanced NMR Spectroscopy of Biomolecules in Frozen Solution. Science. 1997; 276:930. [PubMed: 9139651]
26. Rosay M, Lansing JC, Haddad KC, Bachovchin WW, Herzfeld J, Temkin RJ, Griffin RG. High-Frequency Dynamic Nuclear Polarization in MAS Spectra of Membrane and Soluble Proteins. J Am Chem Soc. 2003; 125:13626–13627. [PubMed: 14599177]
27. Rosay M, Tometich L, Pawsey S, Bader R, Schauwecker R, Blank M, Borchard PM, Cauffman SR, Felch KL, Weber RT, Temkin RJ, Griffin RG, Maas WE. Solid-State Dynamic Nuclear Polarization at 263 GHz: Spectrometer Design and Experimental Results. Phys. Chem. Chem. Phys. 2010; 12:5850–5860. [PubMed: 20449524]
28. Rosay M, Weis V, Kreischer KE, Temkin RJ, Griffin RG. Two-Dimensional 13C-13C Correlation Spectroscopy with Magic Angle Spinning and Dynamic Nuclear Polarization. J Am Chem Soc. 2002; 124:3214–3215. [PubMed: 11916398]
29. Akbey U, Franks WT, Linden A, Lange S, Griffin RG, van RB-J, Oschkinat H. Dynamic Nuclear Polarization of Deuterated Proteins. Angew. Chem., Int. Ed. 2010; 49:7803–7806.
30. Bajaj VS, Mak-Jurkauskas ML, Belenky M, Herzfeld J, Griffin RG. Functional and Shunt States of Bacteriorhodopsin Resolved by 250 GHz Dynamic Nuclear Polarization-Enhanced Solid-State NMR. Proc. Natl. Acad. Sci. U. S. A., Early Ed. 2009:1–6. 6.
31. Mak-Jurkauskas ML, Bajaj VS, Hornstein MK, Belenky M, Griffin RG, Herzfeld J. Energy Transformations Early in the Bacteriorhodopsin Photocycle Revealed by DNP-Enhanced Solid-State NMR. Proc. Natl. Acad. Sci. U. S. A. 2008; 105:883–888. [PubMed: 18195364]
32. Debelouchina GT, Bayro MJ, van d. W. P. C. A. Caporini MA, Barnes AB, Rosay M, Maas WE, Griffin RG. Dynamic Nuclear Polarization-Enhanced Solid-State NMR Spectroscopy of GNNQQNY Nanocrystals and Amyloid Fibrils. Phys. Chem. Chem. Phys. 2010; 12:5911–5919. [PubMed: 20454733]
33. Van der Wel PCA, Hu K-N, Lewandowski J, Griffin RG. Dynamic Nuclear Polarization of Amyloidogenic Peptide Nanocrystals: GNNQQNY, a Core Segment of the Yeast Prion Protein Sup35p. J Am Chem Soc. 2006; 128:10840–10846. [PubMed: 16910679]
34. Bayro MJ, Debelouchina GT, Eddy MT, Birkett NR, MacPhee CE, Rosay M, Maas WE, Dobson CM, Griffin RG. Intermolecular Structure Determination of Amyloid Fibrils with Magic-Angle Spinning and Dynamic Nuclear Polarization NMR. J Am Chem Soc. 2011; 133:13967–13974. [PubMed: 21774549]
35. Maly T, Andreas LB, Smith AA, Griffin RG. 2HDNP-Enhanced 2H-13C Solid-State NMR Correlation Spectroscopy. Physical Chemistry Chemical Physics. 2010; 12:5872–5878. [PubMed: 20458422]
36. Vitzthum V, Caporini MA, Bodenhausen G. Solid-State Nitrogen-14 Nuclear Magnetic Resonance Enhanced by Dynamic Nuclear Polarization Using a Gyrotron. J. Magn. Reson. 2010; 205:177–179. [PubMed: 20488737]
37. Vitzthum V, Mieville P, Carnevale D, Caporini MA, Gajan D, Coperet C, Lelli M, Zagdoun A, Rossini AJ, Lesage A, Emsley L, Bodenhausen G. Dynamic Nuclear Polarization of Quadrupolar Nuclei Using Cross Polarization from Protons: Surface-Enhanced Aluminium-27 NMR. Chem. Commun. 2012; 48:1988–1990.
38. Larsen FH, Jakobsen HJ, Ellis PD, Nielsen NC. QCPMG-MAS NMR of Half-Integer Quadrupolar Nuclei. Journal of Physical Chemistry A. 1997; 101:8597–8606.

NIH-PA Author Manuscript

NIH-PA Author Manuscript

NIH-PA Author Manuscript


39. Kaplan DE, Hahn EL. Experiences de Double Irradiation en Resonande Magnetique par La Methode Dimplusions. Journal de Physique et le Radium. 1958; 19:821–825.
40. Lang DV, Slichter CP, Boyce JB, Lo DC. Measurement of Electron-Spin Density Near Co Atoms in Cu. Phys. Rev. Letters. 1972; 29:776.
41. Abragam, A. Principles of Nuclear Magnetism. Oxford University Press; New York: 2002.
42. Slichter, CP. Principles of Magnetic Resonance. Harper & Row; New York: 1963.
43. Taulelle, F. NMR of Quadrupolar Nuclei in the Solid State. Vol. 322. Kluwer Academic Publishers; London: 1988.
44. Spiess HW, Garrett BB, Sheline RK. Oxygen-17 Quadrupole Coupling Parameters for Water in Its Various Phases. Journal of Chemical Physics. 1969; 51:1201–1205.
45. Michaelis VK, Aguiar PM, Terskikh VV, Kroeker S. Germanium-73 NMR of amorphous and crystalline GeO2. Chemical Communications. 2009; 31:4660–4662. [PubMed: 19641801]
46. O'Dell LA, Schurko RW, Harris KJ, Autschbach J, Ratcliffe CI. Interaction Tensors and Local Dynamics in Common Structural Motifs of Nitrogen: A Solid-State 14N NMR and DFT Study. Journal of the American Chemical Society. 2011; 133:527–546.
47. Widdifield CM, Bryce DL. Solid-State Br-79/81 NMR and Gauge-Including Projector-Augmented Wave Study of Structure, Symmetry, and Hydration State in Alkaline Earth Metal Bromides. Journal of Physical Chemistry A. 2010; 114:2102–2116.
48. Cheng JT, Ellis PD. Adsorption of Rb+ to Gamma-Alumina as Followed by Solid-State Rb-87 NMR-Spectroscopy. Journal of Physical Chemistry. 1989; 93:2549–2555.
49. Rossini AJ, Zagdoun A, Lelli M, Gajan D, Rascon F, Rosay M, Maas WE, Coperet C, Lesage A, Emsley L. One Hundred Fold Overall Sensitivity Enhancements for Silicon-29 NMR Spectroscopy of Surfaces by Dynamic Nuclear Polarization with CPMG Acquisition. Chem. Sci. 2012; 3:108–115.
50. Hu K-N, Yu H-H, Swager TM, Griffin RG. Dynamic Nuclear Polarization with Biradicals. J Am Chem Soc. 2004; 126:10844–10845. [PubMed: 15339160]
51. Song C, Hu K-N, Joo C-G, Swager TM, Griffin RG. TOTAPOL – A Biradical Polarizing Agent for Dynamic Nuclear Polarization Experiments in Aqueous Media. J. Am Chem. Soc. 2006; 128:11385–11390. [PubMed: 16939261]
52. Bak M, Rasmussen JT, Nielsen NC. J. Magn. Reson. 2000; 147:296. [PubMed: 11097821]
53. Sachleben JR, Frydman V, Frydman L. Dipolar Determinations in Solids by Relaxation-Assisted NMR Recoupling. Journal of the American Chemical Society. 1996; 118:9786–9787.
54. Barnes AB, De PG, van d. W. P. C. A. Hu KN, Joo CG, Bajaj VS, Mak-Jurkauskas ML, Sirigiri JR, Herzfeld J, Temkin RJ, Griffin RG. High-Field Dynamic Nuclear Polarization for Solid and Solution Biological NMR. Appl. Magn. Reson. 2008; 34:237–263. [PubMed: 19194532]
55. Veshtort M, Griffin RG. SPINEVOLUTION: A Powerful Tool for Simulations of Solid and Liquid State NMR Experiments. J. Magn. Resonance. 2006; 178:248–282.
56. Bilalbegovic G. Nuclear Magnetic Resonance Parameters of Water Hexamers. The Journal of Physical Chemistry A. 2009; 114:715–720. [PubMed: 20020771]
57. Fortes AD, Wood IG, Grigoriev D, Alfredsson M, Kipfstuhl S, Knight KS, Smith RI. No Evidence for Large-Scale Proton Ordering in Antarctic Ice from Powder Neutron Diffraction. Journal of Chemical Physics. 2004; 120:11376–11379. [PubMed: 15268170]
58. Kuhs WF, Lehmann MS. Bond-Lenghts, Bond Angles and Transition Barrier in Ice IH by Neutron-Scattering. Nature. 1981; 294:432–434.
59. van Beek JD, Dupree R, Levitt MH. Symmetry-Based Recoupling of 17O-1H Spin Pairs in Magic-Angle Spinning NMR. J. Magn. Reson. 2006; 179:38–48. [PubMed: 16309936]
60. Van Eck ERH, Smith ME. Orientation of the Quadrupole and Dipole Tensors of Hydroxyl Groups by O-17 Quadrupole Separated Local Field NMR. J. Chem. Phys. 1998; 108:5904–5913.
61. Linder M, Hohener A, Ernst RR. Orientation of Tensorial Interactions Determined from 2-Dimensional NMR. Powder Spectra Journal of Chemical Physics. 1980; 73:4959–4970.
62. Pike KJ, Lemaitre V, Kukol A, Anupold T, Samoson A, Howes AP, Watts A, Smith ME, Dupree R. Solid-State 17O NMR of Amino Acids. J. Phys. Chem. B. 2004; 108:9256–9263.

NIH-PA Author Manuscript

NIH-PA Author Manuscript

NIH-PA Author Manuscript

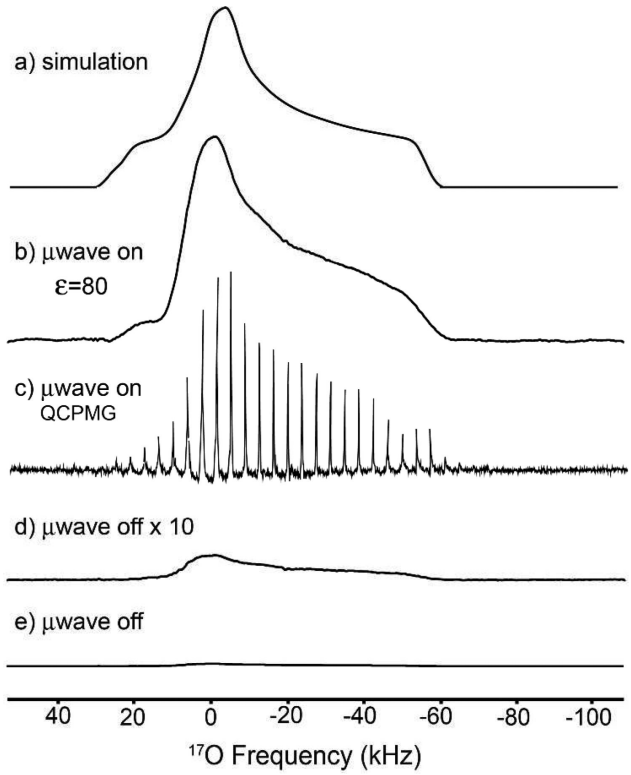


**Figure 1.**

Central transition $^{17}O$-$^{1}H$ cross-polarization-echo of a static glycerol/$D_2O$/$H_2{}^{17}O$ (60/30/10 % by weight) recorded at T = 82 K in which the water was originally 74% enriched in $H_2{}^{17}O$. The final concentration of $H_2{}^{17}O$ was ~7.4%: (a) lineshape simulation, (b) wave on with ε~80 (128 scans), (c) μwave on using a CPMG (16 scans), (d) wave off scaled by 10 and (e) wave off (4864 scans).

NIH-PA Author Manuscript
NIH-PA Author Manuscript
NIH-PA Author Manuscript



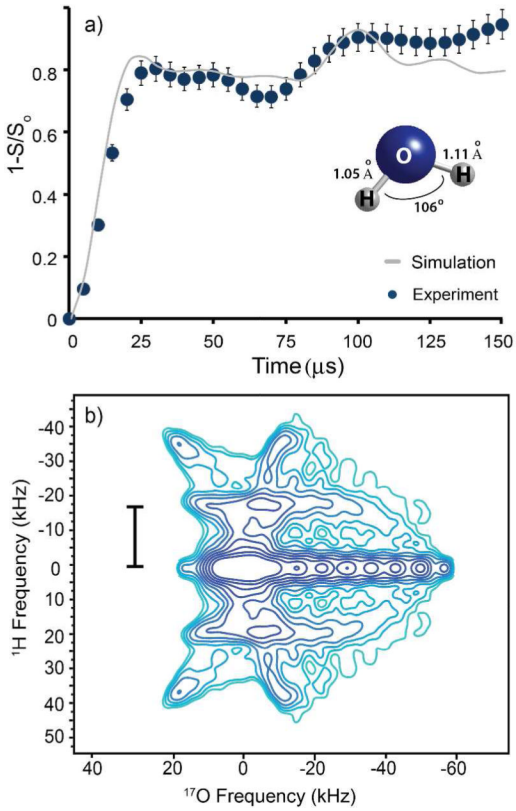


**Figure 2.**

Central transition $^{17}$O-$^{1}$H SEDOR experiment recorded at T=85 K using 74% enriched in $^{17}$O: (a) SEDOR curve with SIMPSON simulation and (b) 2D SEDOR spectrum. The sample composition is as in Figure 1.

NIH-PA Author Manuscript
NIH-PA Author Manuscript
NIH-PA Author Manuscript



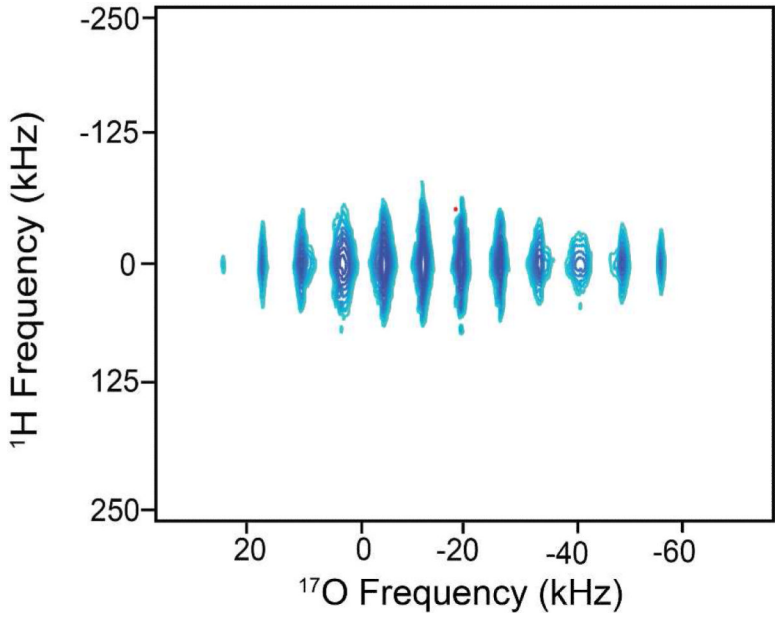


**Figure 3.**
Central transition $^{17}$O-$^{1}$H HETCOR-CPMG spectrum of water/glycerol glass using solid-state DNP NMR, T=85 K. The sample composition is as in Figure 1.